

THE MICROMECHANICS OF THE MOVING CONTACT LINE

Seth Lichter, Department of Mechanical Engineering, Northwestern University, Evanston, IL 60208-3111
s-lichter@nwu.edu

ABSTRACT

A transient moving contact line is investigated experimentally. The dynamic interface shape between $20\mu\text{m}$ and $800\mu\text{m}$ from the contact line is compared with theory. A novel experiment is devised, in which the contact line is set into motion by electrically altering the solid-liquid surface tension γ_{SL} . The contact line motion simulates that of spontaneous wetting along a vertical plate with a maximum capillary number $Ca \sim 4 \cdot 10^{-2}$. The images of the dynamic meniscus are analyzed as a function of Ca . For comparison, the steady-state hydrodynamic equation based on the creeping flow model in a wedge geometry and the three-region uniform perturbation expansion of Cox (1986) is adopted. The interface shape is well depicted by the uniform solution for $Ca \leq 10^{-3}$. However, for $Ca > 10^{-3}$, the uniform solution over-predicts the viscous bending. This over-prediction can be accounted for by modifying the slip coefficient within the intermediate solution. With this correction, the measured interface shape is seen to match the theoretical prediction for all capillary numbers. The amount of slip needed to fit the measurements does not scale with the capillary number.

Introduction

In this work, we seek to model spontaneous wetting. The experimental method to mimic spontaneous wetting makes use of electrical double layer theory. Experimental results are compared to an asymptotic theory [1] which describes the shape of the fluid interface. One of the objectives of this work is to assess the utility of this theory to the case of spontaneous wetting. Rigorous testing comparing theory and experiment has already been done for controlled wetting in which the contact line moved at constant capillary number [2, 3]. We find here that for flows with a suitably low maximum capillary, steady theory is applicable. However, for flows at higher capillary number, the measurements deviate from theoretical values. The source of this discrepancy does not appear to be due to the unsteadiness of the spontaneous wetting flow. Rather, it appears to be due to a large region of slip which invalidates theory's assumption that slip is of more limited extent.

Surface Tension Depends on Electrical Potential

In a container filled with fluid and vapor, the location where the fluid/vapor interface meets the solid container is denoted as the contact line, see Fig. 1. Young's equation

$$\gamma_{SV} = \gamma_{SL} + \gamma_{LV} \cos \theta,$$

relates the the surface tension at the solid/vapor (SV) interface to that along the solid/liquid (SL) and liquid/vapor (LV) interfaces as well as to the contact angle θ . It can also be shown [4] that

$$\left(\frac{\partial \gamma_{SL}}{\partial V_M} \right) = -\sigma_o,$$

which reveals that the surface tension at the solid/liquid interface can be modified by an applied potential V_M to the wetted solid surface; σ_o is the surface charge density. If we denote the maximum surface tension when $\sigma_o = 0$ as γ_{SL}^o , and the corresponding potential as V_o , then the above equation gives

$$\gamma_{SL} = \gamma_{SL}^o - \int_{V_o}^{V_M} \sigma_o dV.$$

The integral on the right-hand side is the electrical energy stored in the double layer at the solid/liquid interface. If we now estimate the double layer energy in terms of the Helmholtz model [5], then

$$\gamma_{SL} = \gamma_{SL}^o - \int_{V_o}^{V_M} CV dV,$$

where C is the capacitance of the double layer. Carrying out the integration yields,

$$\gamma_{SL} = \gamma_{SL}^o - \frac{C}{2} (V_M - V_o)^2.$$

The above equation provides an operational equation for the manipulation of solid-liquid surface tension. The application of a potential will alter the solid/liquid surface tension γ_{SL} ; consequently, the balance of Young's equation is disrupted; the contact line then must move to a new location at which a new angle θ is established as a new equilibrium angle.

Experiment

Contact line motion takes place on a gold-mercury (Au-Hg) amalgam surface. The liquid used is a mixture of

glycerol and water to which a bit of KOH is added to enhance conductivity. A step change in surface potential is applied by a computer controlled potentiostat. The subsequent motion of the contact line is observed using a CCD camera attached to a microscope, see Fig. 2.

Asymptotic Theory

An asymptotic theory has been developed which describes the shape of the liquid/vapor interface as a function of distance from the contact line [1, 6, 7]. The interface shape is expressed in terms of the local interface angle

$$\theta = \left(\theta_d^3 + 9Ca \ln \frac{r}{L_{cap}} \right)^{1/3} + f(r) - \theta_d, \quad (1)$$

and where θ_d is the apparent contact angle, Ca is the capillary number, $L_{cap} \equiv \sqrt{2\gamma_{LV}/\rho g}$ is the capillary length, and $f(r)$ is the static shape of the interface in the absence of motion, see Fig. 1.

Experimental Results

In response to the application of a potential V_M , the contact line is set into motion. The measured capillary number as a function of time is shown in Fig. 3. At first, the contact line moves at high capillary number and, as time proceeds, it slows down. At any selected time, that is, at any capillary number, the interface shape can be determined from the images gathered by the CCD camera, for example as shown in Fig. 4. The difference between the observed interfacial angle θ and that given by the theory of Eq. (1) can be computed, as shown in Fig. 5. In this particular figure, the agreement between the theory and measurement stretches from about $200\mu\text{m} < x < 470\mu\text{m}$. This pair of minimum and maximum values bound the interval over which the theory and experiment agree. This pair of values is gathered for an entire run in Fig. 6. While for $Ca \lesssim 5 \cdot 10^{-3}$, the theory and experiment agree over the entire field of view, at higher capillary numbers, the interval of agreement narrows. Finally, at $Ca \approx 4 \cdot 10^{-2}$, the interval of agreement has narrowed to zero.

Modified Theoretical Model

The theoretical results shown in Eq. (1) were derived under the condition that slip occurs within a molecular-sized region at the contact line. If slip is allowed over a much longer extent, then an *ad hoc* analysis shows that the theory is modified,

$$\theta = \left(\theta_d^3 + 9\beta Ca \ln \frac{r}{L_{cap}} \right)^{1/3} + f(r) - \theta_d, \quad (2)$$

where the factor β , which appears on the right-hand side of the equation, is a measure of slip at intermediate length scales. If $\beta = 1$, then the original model is recovered. If $\beta = 0$, then slip occurs over the entire intermediate region. By fitting β , it is found that the interval over which the measurement and the modified theory, Eq. (2), agree can be made to extend over the entire field of view, see Fig. 7.

Conclusion

This work investigates spontaneous wetting. A flow which mimics spontaneous wetting is established by utilizing the variation of solid/liquid surface tension with the potential applied at the solid surface. It is found that the steady asymptotic theory holds for low values of the capillary number, even though the flow is unsteady. At higher values of the capillary number, agreement between theory and experiment fails. The discrepancy may be due to slip occurring over a large interval of the solid/liquid interface.

ACKNOWLEDGMENTS

This work has been supported by the NASA Microgravity Science and Applications Division under grant NAG3-1892. I would like to thank the Technical Officer, Dr. Mark Weislogel, for his years of advice and encouragement. The help of Chih-Yu Lin in preparing this paper is gratefully acknowledged.

REFERENCES

References

- [1] R. G. Cox. The dynamics of the spreading of liquids on a solid surface. Part 1. Viscous flow. *J. Fluid Mech.*, 168:169--194, 1986.
- [2] Q. Chen, E. Ramé, and S. Garoff. The breakdown of asymptotic hydrodynamic models of liquid spreading at increasing capillary number. *Phys. Fluids*, 7:2631--2639, 1995.
- [3] E. Ramé and S. Garoff. Microscopic and macroscopic dynamic interface shapes and the interpretation of dynamic contact angles. *J. Colloid Int. Sci.*, 177:234--244, 1996.
- [4] J. T. Davies and E. K. Rideal. *Interfacial Phenomena*. Academic Press, 1963.
- [5] Y. Y. Perng. *The unsteady moving contact line: Experimental investigation*. PhD thesis, Northwestern University, 1998.
- [6] E. B. Dussan V, E. Ramé, and S. Garoff. On identifying the appropriate boundary conditions at a moving contact line: an experimental investigation. *J. Fluid Mech.*, 230:97--116, 1991.
- [7] A. J. J. van der Zanden. *The hydrodynamics of a moving fluid-liquid contact line*. PhD thesis, Technische Universiteit Eindhoven, 1993.

REFERENCES

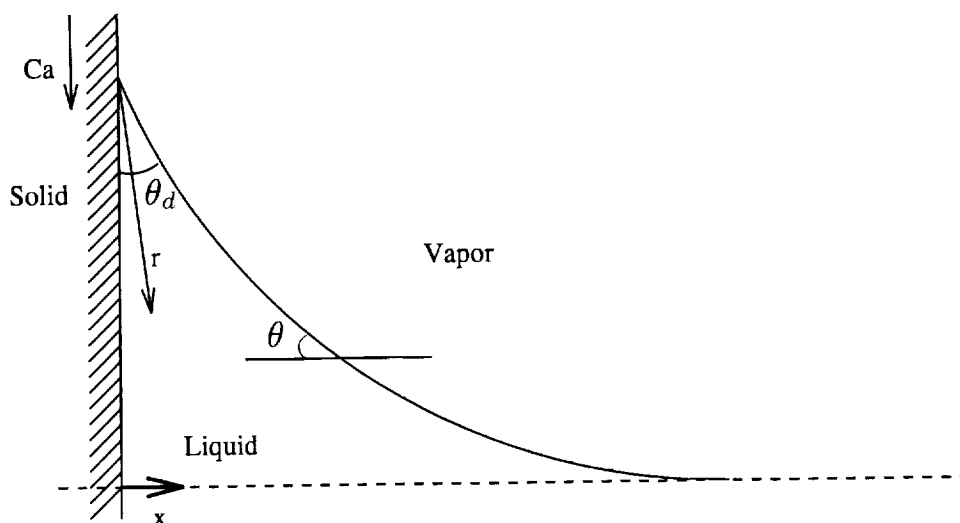


Figure 1: The moving contact line. For an advancing contact line, the wall moves relative to the fluid as shown, characterized by the capillary number Ca . In spontaneous wetting, the capillary number is a function of time. The local angle θ varies along the interface.

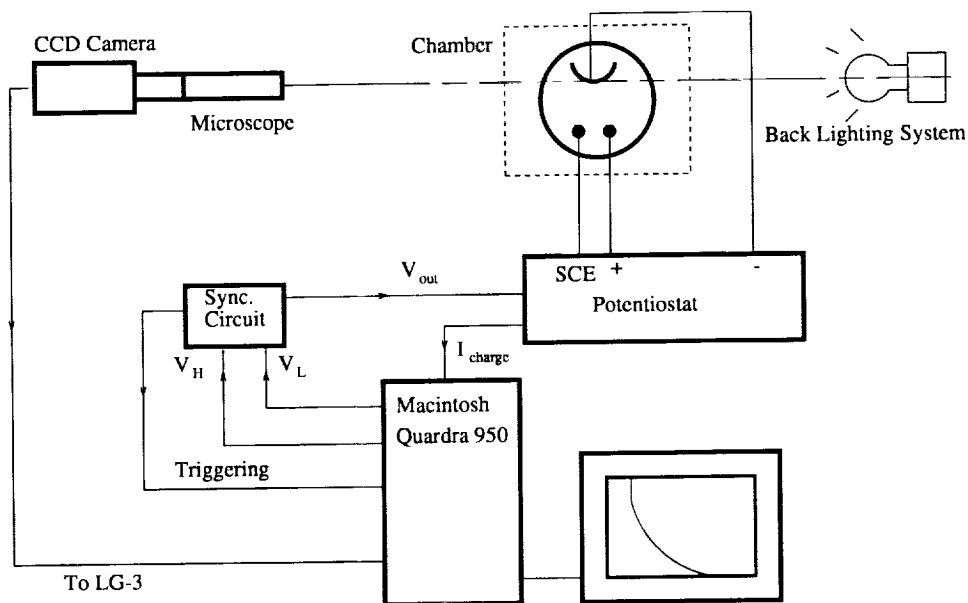


Figure 2: Schematic of the experimental set-up. The curved Au-Hg plate is immersed in KOH solution in the experimental chamber, here seen in top view. The two dots in the chamber are electrodes which apply a step change in potential to the plate. After processing, the CCD camera produces a view of the interface, as sketched here on the monitor. From this view, the interface shape can be determined.

REFERENCES

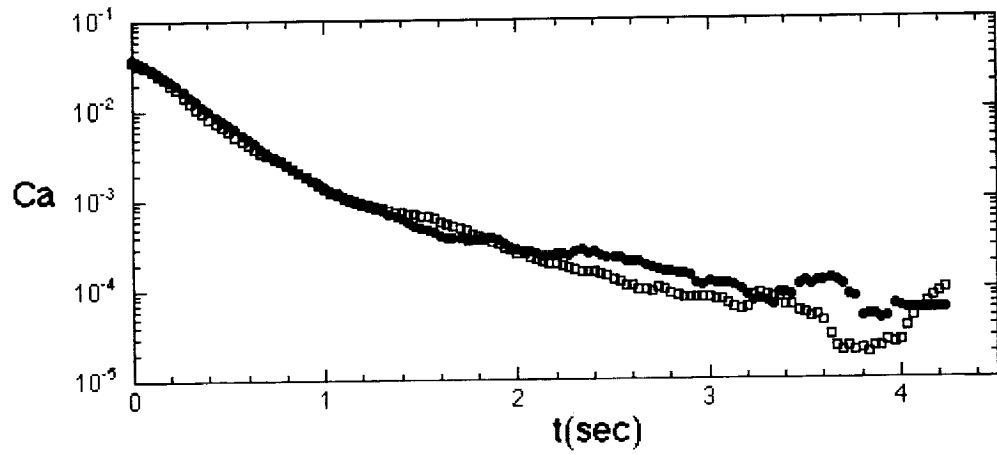


Figure 3: The capillary number as a function of time after a step change in potential is applied to the plate. Data from two runs is shown. The scatter for times greater than about 3 seconds is due to inaccuracies in measuring these low capillary numbers.

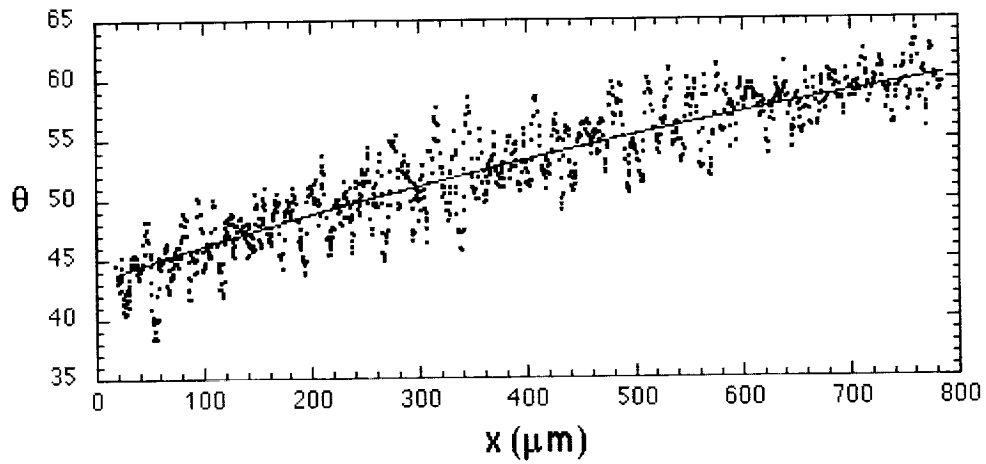


Figure 4: Dynamic profile for $Ca \sim 1.58 \cdot 10^{-3}$. Dots are data and the solid curve is the outer solution $f(r)$, see Eq. (1).

REFERENCES

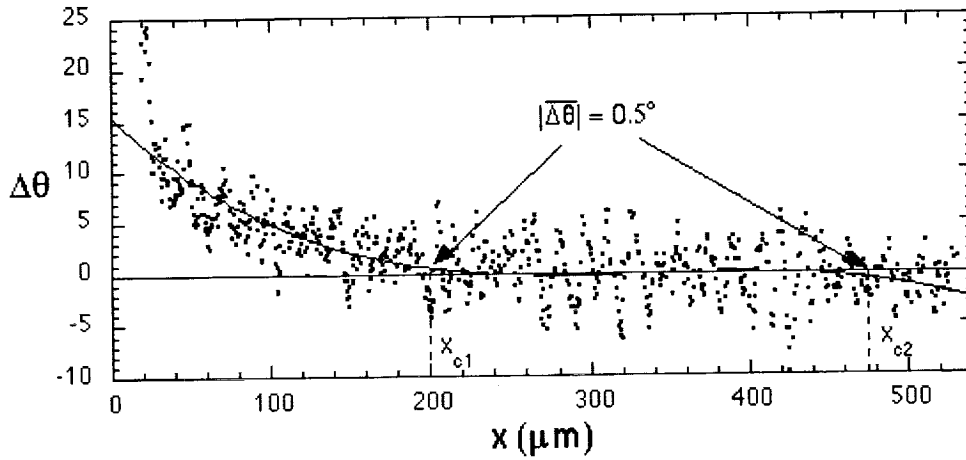


Figure 5: Difference between the measurement of interface angle and the prediction from Eq. (1) for $Ca \sim 2.06 \cdot 10^{-2}$. The equation and measurement agree over the interval in x between the dashed lines.

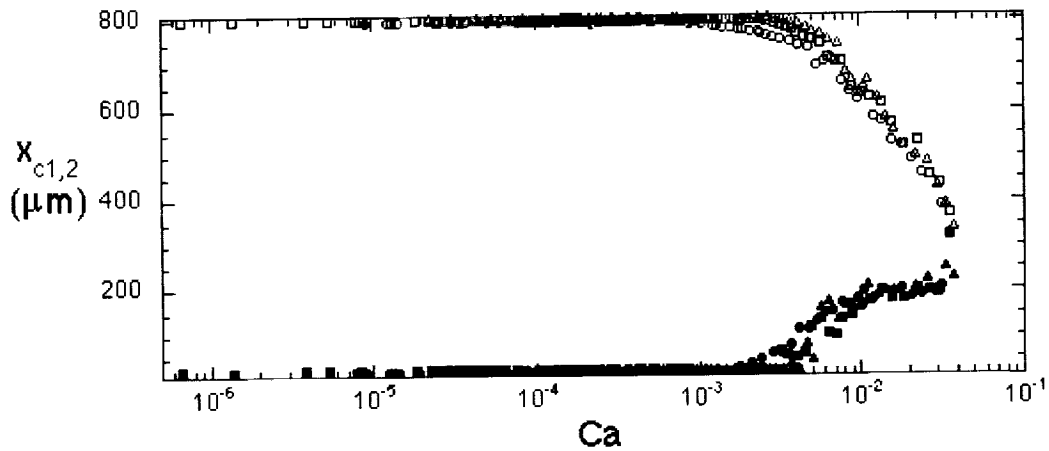


Figure 6: The extent of agreement between theory, Eq. (1), and experiment for one run. Data such as shown in Fig. 5 define the maximum (minimum) distance from the wall at which agreement is found, shown here by the open (closed) symbols. The x -distance between the symbols indicates the interval of agreement. At low capillary numbers, the agreement stretches over the entire field of view. At higher capillary numbers, the interval of agreement narrows. At the highest capillary number shown, there is no interval in which theory and measurement agree.

REFERENCES

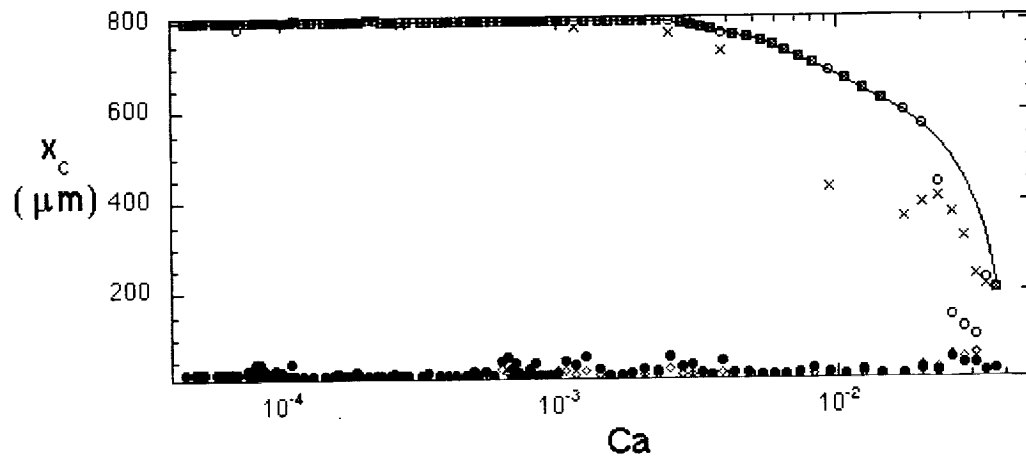


Figure 7: A similar figure to Fig. 6, however here the data is compared with the modified theory, Eq. (2). The maximum (minimum) distance from the wall at which agreement is found, is shown here by the open (closed) symbols. The line shows the outer location of the field of view. Note that for $Ca > 5 \cdot 10^{-3}$ by using the modified theory the interval of agreement is larger than that found using Eq. (1), shown in Fig. 6.